Environmental Research Letters

LETTER

Significant feedbacks of wetland methane release on climate change and the causes of their uncertainty

N Gedney[1,4] , C Huntingford[2], E Comyn-Platt[2] and A Wiltshire[3]

[1] Met Office Hadley Centre, Joint Centre for Hydrometeorological Research, Maclean Building, Wallingford OX10 8BB, United Kingdom
[2] Centre for Ecology and Hydrology, Wallingford OX10 8BB, United Kingdom
[3] Met Office Hadley Centre, FitzRoy Road, Exeter, EX1 3PB, United Kingdom
[4] Author to whom any correspondence should be addressed.

E-mail: nicola.gedney@metoffice.gov.uk

Abstract

Emissions from wetlands are the single largest source of the atmospheric greenhouse gas (GHG) methane (CH_4). This may increase in a warming climate, leading to a positive feedback on climate change. For the first time, we extend interactive wetland CH_4 emissions schemes to include the recently quantified, significant process of CH_4 transfer through tropical trees. We constrain the parameterisations using a multi-site flux study, and biogeochemical and inversion models. This provides an estimate and uncertainty range in contemporary, large-scale wetland emissions and their response to temperature. To assess the potential for future wetland CH_4 emissions to feedback on climate, the schemes are forced with simulated climate change using a 'pattern-scaling' system, which links altered atmospheric radiative forcing to meteorology changes. We perform multiple simulations emulating 34 Earth System Models over different anthropogenic GHG emissions scenarios (RCPs). We provide a detailed assessment of the causes of uncertainty in predicting wetland CH_4–climate feedback. Despite the constraints applied, uncertainty from wetland CH_4 emission modelling is greater that from projected climate spread (under a given RCP). Limited knowledge of contemporary global wetland emissions restricts model calibration, producing the largest individual cause of wetland parameterisation uncertainty. Wetland feedback causes an additional temperature increase between 0.6% and 5.5% over the 21st century, with a feedback on climate ranging from 0.01 to 0.11 $Wm^{-2} K^{-1}$. Wetland CH_4 emissions amplify atmospheric CH_4 increases by up to a further possible 25.4% in one simulation, and reduce remaining allowed anthropogenic emissions to maintain the RCP2.6 temperature threshold by 8.0% on average.

Introduction

CH_4 is the second largest contributor to the anthropogenic greenhouse gas (GHG) effect after carbon dioxide (CO_2), contributing about 21% of the increased radiative forcing since pre-industrial times (Myhre *et al* 2013). Over a 100 year time period CH_4 global warming potential is about 28 times that of CO_2 (Myhre *et al* 2013). Surface atmospheric CH_4 concentrations reached 1810 ppb in 2012 (Saunois *et al* 2016), which is about 2.5 times as large as pre-industrial concentrations. In the late 1990s and early 2000s there was a near decade of minimal growth in atmospheric CH_4, which has recently been followed by a renewed and sustained period of increase (Nisbet *et al* 2014).

Natural wetland emissions currently contribute up to approximately 40% of the global CH_4 emissions total (Saunois *et al* 2016), and are thought to cause much of the yearly atmospheric CH_4 concentration variability (McNorton *et al* 2016). These emissions are expected to produce a positive feedback on climate change (Gedney *et al* 2004, Arneth *et al* 2010, Ciais *et al* 2013, Melton *et al* 2013, Stocker *et al* 2013) but are assessed to have a 'very low' scientific confidence (Arneth *et al* 2010).

The Saunois *et al* (2016) review shows that present-day wetland CH_4 global emissions remain highly uncertain, though there is some consistency between estimates using top-down (atmospheric inversions which incorporate observations into dynamic and chemistry models) and bottom-up (process-based land models) approaches, with ranges of 127–202 $TgCH_4yr^{-1}$ and 153–227 $TgCH_4yr^{-1}$, respectively. The range in bottom-up estimates of Saunois *et al* (2016) is smaller than reported in similar earlier studies (Kirschke *et al* 2013, Melton *et al* 2013), which is mainly due to the use of a common wetland area map across models.

Amazon basin observations have recently found that tropical trees act as significant conduits for wetland CH_4 emissions (Pangala *et al* 2017), transferring about half of the total wetland flux here. These measurements have resolved the previously large discrepancy between CH_4 flux estimates from scaled-up flux measurements and top-down approaches over this large regional source (Pangala *et al* 2017). However, lack of detailed knowledge of present-day wetland extent remains a large contributor to current emissions uncertainty in process-based models, as it is often used for scaling up (Kirschke *et al* 2013, Saunois *et al* 2016). Uncertainties in atmospheric chemistry and transport, and non-wetland CH_4 budgets contribute significantly to inversion model estimate uncertainty (Saunois *et al* 2016).

From a limited number of studies over different climate change scenarios, global wetland CH_4 emissions are projected to increase by up to 78% (with simulated climate change between present day and doubling of atmospheric CO_2), and enhanced future feedback raises radiative forcing by up to 0.1 $Wm^{-2}K^{-1}$ (Arneth *et al* 2010, Ciais *et al* 2013). To extend this we take a more rigorous approach in assessing CH_4 wetland feedback under climate change. We consider separate parameterisations of the two primary wetland CH_4 generation processes, include CH_4 transfer through trees and a new representation of tropical soils, and adopt better constrained parameters. We then apply this in a framework of multiple emissions scenarios and 34 different Earth System Models (ESM) climate change estimates.

JULES wetland model

CH_4 consumption (methanotrophy) in the non-saturated zone above the water table is far more efficient than methanogenesis occurring within the saturated zone (Roulet *et al* 1992). Hence we assume that CH_4 produced in the soil saturated zone can only reach the atmosphere directly when the water table reaches the soil surface (incorporated via the grid-box wetland fraction; Gedney *et al* 2004). CH_4 in the soil saturated zone may still be transferred to the atmosphere via vegetation when the water table is lower

however. With emissions being so dependent on water table depth, it is necessary to simulate hydrology and wetland extent adequately.

Large-scale surface models traditionally use soil hydraulic properties based on sand, silt and clay percentages (Best *et al* 2011). In order to improve the hydrological depiction in the tropics, which is a major contributor to the global wetland CH_4 budget, we extend our soil properties to include tropical soils (ferralsols, which are weathered soils with micro-aggregated particles), as these are poorly represented by standard particle distribution functions (Marthews *et al* 2014).

JULES (Clark *et al* 2011) simulates the wetland fraction *fw* by combining simulated grid-box mean water table depth and sub-grid topographic distribution to produce a sub-grid water table depth distribution *fw'(z)* (supplementary appendix SA is available online at stacks.iop.org/ERL/14/084027/mmedia). *fw* is defined as the grid-box fraction where the water table is at or just above the surface *zwet*, i.e. $fw = \int_0^{zwet} fw'(z)\,dz$ (Gedney *et al* 2004, Gedney and Cox 2003). Thus *fw* can be compared against observation-based inundation products.

To incorporate CH_4 transfer through vegetation, including the significant flux via tropical trees (Pangala *et al* 2017), we extend the standard modelled *fw* to include an *effective* wetland extent *fwe*. We assume this flux through vegetation can occur where roots exist below the water table. The flux originating at soil depth *z* is therefore proportional to the relative occurrence of water table depth at *z* within the grid box *fw'(z)*, and the fractional number of roots below *z*, *P(z)*. Root distribution decays exponentially up to total soil depth z_{soil}, according to root depth z_r:

$$P(z) = \frac{\int_{z_{soil}}^{z} e^{-\frac{z}{z_r}}\,dz}{z_r(1 - e^{-\frac{z_{soil}}{z_r}})}. \qquad (1)$$

Integrating *P(z)fw'(z)* gives:

$$\int_{z_{soil}}^{zwet} P(z)fw'(z)\,dz = \int_{z_{soil}}^{0} P(z)fw'(z)\,dz + fw$$

as $\int_{z_{soil}}^{0} P_i(z)\,dz = 1$ by definition. Summing over vegetation fractions fv_i, we obtain an *effective* vegetation wetland fraction fwe_v which encompasses vegetation transfer:

$$fwe_v = \sum_i fv_i.A\left[\int_{z_{soil}}^{0} P_i(z)fw'(z)\,dz + fw\right].$$

Here *i* represents each vegetation type. Efficiency factor *A* relates to how effectively CH_4 is removed from the soil via vegetation. Over vegetation when the water table is at or above the surface, we assume that any soil CH_4 not lost through vegetation is emitted directly into the atmosphere. Hence the effective wetland fraction for soil is:

$$fwe_s = \sum_i fv_i . (1 - A)fw + \left(1 - \sum_i fv_i\right). fw.$$

Due to lack of detailed, available measurements, such as how vegetation flux varies with water table depth, A can only be calculated by ensuring the total fraction of CH_4 emitted via tropical Amazon trees agrees with that observed (∼0.5; Pangala *et al* 2017). Since Pangala *et al* (2017) is the only comprehensive, large-scale study on this (Covey and Megonigal 2019) we assume that the tuned 'A' value is valid over all vegetation types. Applying this 'A' value to different plant functional types is non-ideal, however its impact on total flux over other vegetation types is small partially due to shallower rooting depths. (Figure S5 shows that including vegetation transfer has little effect outside tropical South America). This finding is consistent with McNorton *et al* (2016), which shows that incorporating additional processes, such as CH_4 transport via short vegetation, does not improve overall CH_4 flux simulation.

JULES CH$_4$ parameterisation

CH_4 production in wetlands occurs via two main pathways: acetoclastic and hydrogenotrophic methanogenesis. Acetic acid from root exudates (related to net primary productivity NPP; Bridgham *et al* 2013) is the substrate for the former, whereas CO_2 from the soil carbon store is a source for the latter. There is considerable uncertainty about the relative importance of the two substrates in CH_4 generation at the large-scale however, causing speculation that this is a large contributory factor in future wetland CH_4 flux uncertainty (Bridgham *et al* 2013). To place bounds on this uncertainty, JULES is run with two CH_4 parameterisations, where the source for wetland CH_4 flux into the atmosphere (F_{CH4}) is based on either soil carbon Cs (kgm^{-2}) or NPP ($kgm^{-2}\,s^{-1}$). Due to the inclusion of vegetation-mediated flux, total CH_4 fluxes become dependent on an effective wetland fraction, fwe (where $fwe = fwe_s + fwe_v$):

$$F_{CH4}(Cs) = fwe .K_{CS} .Cs. Q10_{CS}(T)^{\frac{T-To}{10}}, \quad (2)$$

$$F_{CH4}(NPP) = fwe.K_{NPP} .NPP. Q10_{NPP}(T)^{\frac{T-To}{10}}, \quad (3)$$

where $T(K)$ is the mean top 1 m soil temperature and To a reference temperature (273.16 K). $F_{CH4}(NPP)$ is restricted from going below zero, as would otherwise occur if NPP becomes negative. (Soil uptake is included within the atmospheric methane lifetime). The choice of two substrates is important, as they are likely to have different climate sensitivities: $F_{CH4}(Cs)$ is proportional to a large pool, which we assume is time invariant; $F_{CH4}(NPP)$ is sensitive to a change in flux, with initial soil CH_4 emissions occurring less than twelve hours after photosynthetic assimilation (Megonigal *et al* 1999). Both schemes are sensitive to

climate through their $Q10$ temperature relationships and effective wetland fraction (fwe), with $F_{CH4}(NPP)$ having an additional substrate sensitivity to climate and atmospheric CO_2. These two schemes are chosen to see if uncertainties in the temporal production of available substrate is important in the climate-CH_4 feedback response.

K_{CS} and K_{NPP} are tuned to produce the appropriate global total wetland flux to cover the total range for all models in Saunois *et al* (2016), 127–227 $TgCH_4yr^{-1}$. (K_{CS} varies from 3.2–5.0 × $10^{-12}\,s^{-1}$ and K_{NPP} 4.1–8.0 × 10^{-3} (unitless) from UPP to LOW). $Q10(T)$ factors in equations (2) and (3) describe the amounts by which reaction rates increase with a 10 K temperature increase. These factors are themselves a function of temperature, so as to directly follow the Arrhenius equation which describes the temperature dependence of a biological process. Thus using a temperature dependent $Q10$ allows us to fit the Arrhenius equation beyond a specific climatic region. Hence $Q10(T) = Q10_{To}^{To/T}$, where $Q10_{To}$ is the $Q10$ temperature sensitivity at To. $Q10_{CS,To}$ and $Q10_{NPP,To}$ are specific to the methanogenesis pathways considered.
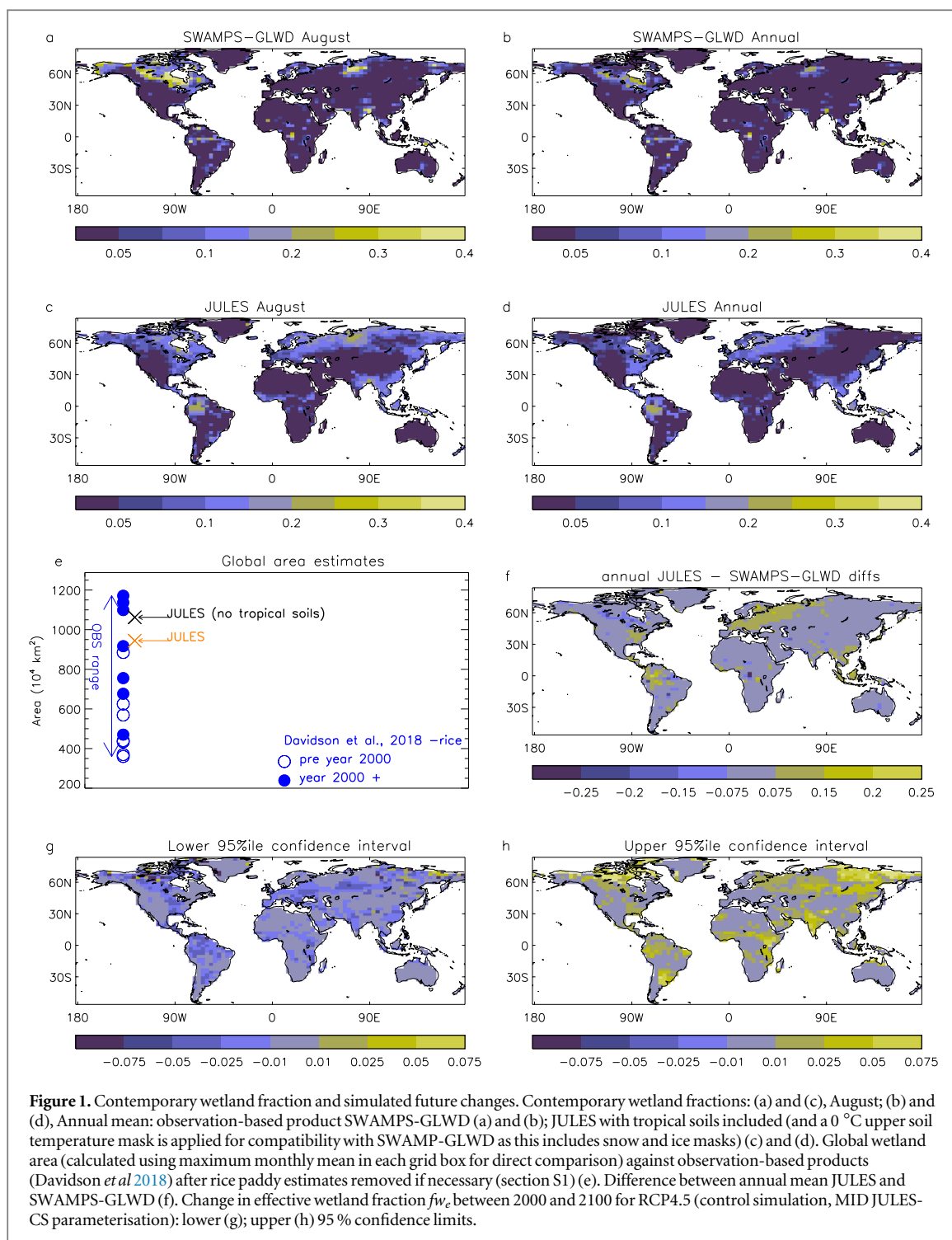
The above scheme does not include some more detailed processes, such as CH_4 suppression due to sulphate deposition, some transport mechanisms, and multiple CH_4 pools. McNorton *et al* (2016) demonstrate that their inclusion does not improve overall model performance, and there are insufficient observations to adequately constrain many such processes (e.g. redox and pH, Riley *et al* 2011). Instead we focus on constraining temperature sensitivity using a large number of observations over an extensive number of field sites (Turetsky *et al* 2014), as uncertainty in temperature response has the largest impact on net CH_4 emissions (Riley *et al* 2011).

JULES wetland and CH$_4$ calibration and validation

In order to calibrate the JULES wetland CH_4 relations (JULES-CS, JULES-NPP) off-line runs are carried out using observation-based meteorology (Weedon *et al* 2014) at 0.5° resolution for all land points.

The wetland fraction simulated by JULES compares well spatially (figure 1) and temporally (figure S2) with the SWAMPS-GLWD (Poulter *et al* 2017) observation-based product, and is within observational spread for global total wetland area (figure 1(e), Davidson *et al* 2018). A detailed assessment of simulated wetland uncertainty and its impact on the magnitude of wetland CH_4 feedback on climate change is provided in the supplementary material SI sections S1 and S7.

To calibrate the soil carbon-based emission relation JULES-CS, temperature sensitivity $Q10_{To,CS}$ is determined by fitting against $Q10$'s in the multiple wetland site data analysis (Turetsky *et al* 2014, $Q10_{Tur}$,

Figure 1. Contemporary wetland fraction and simulated future changes. Contemporary wetland fractions: (a) and (c), August; (b) and (d), Annual mean: observation-based product SWAMPS-GLWD (a) and (b); JULES with tropical soils included (and a 0 °C upper soil temperature mask is applied for compatibility with SWAMP-GLWD as this includes snow and ice masks) (c) and (d). Global wetland area (calculated using maximum monthly mean in each grid box for direct comparison) against observation-based products (Davidson *et al* 2018) after rice paddy estimates removed if necessary (section S1) (e). Difference between annual mean JULES and SWAMPS-GLWD (f). Change in effective wetland fraction fw_e between 2000 and 2100 for RCP4.5 (control simulation, MID JULES-CS parameterisation): lower (g); upper (h) 95 % confidence limits.

section S2). To directly map $Q10_{To,CS}$ onto $Q10_{Tur}$, JULES-CS must use *fixed* (observed) soil carbon (Nachtergaele and Batjes 2012), which is equivalent to assuming a highly recalcitrant and/or large soil carbon pool that changes negligibly over time. Using this fitting procedure we produce lower (LOW), mid (MID) and upper (UPP) estimates of $Q10_{CS,To}$ of 3.0, 3.7 and 4.7 (equivalent to poor and rich fens, and bogs in Turetsky *et al* 2014), respectively (SI table S1).

The intermediate $Q10_{CS,To}$ value of 3.7 obtained from the above bottom-up approach here is very close to that found in Gedney and Cox (2003) (3.4–3.7),

where the CH_4 parameterisation was calibrated against global inter-annual variations in atmospheric CH_4 (a top-down approach). Although Turetsky *et al* (2014) focuses on bogs and fens, Yvon-Durocher *et al* (2014) demonstrate that for multiple eco-systems spanning the globe, CH_4 emissions have a consistent mean temperature dependence (0.96 eV with a 95% confidence of 0.86–1.07 eV). This is numerically equivalent to $Q10_{To} = 4.5$ and range of 3.8–5.3 (as 1 eV $\sim 1.6 \times 10^{-19}$ J), and consistent with our estimates of 3.0–4.7. The resulting regional distribution of JULES CH_4 fluxes compare well against other

estimates (Saunois *et al* 2016, section S4). The Amazon basin emissions and uncertainty ranges produced by JULES also compare well with estimates extrapolated from a large-scale measurement campaign (JULES: 24.6–53.9, Pangala *et al* 2017: 24.4–53.5 TgCH$_4$yr^{-1}; table S2). (As we have tuned the tree-mediated fluxes to be 50% of the total, and our flux totals agree with observations, it follows that there is also good agreement between the tree-mediated fluxes: JULES 12.3–27.0, Pangala *et al* 2017 11.5–26.2 TgCH$_4$yr^{-1}). The aforementioned comparisons demonstrate consistency across very different calibration approaches and different spatial and temporal scales, indicating that $Q10_{CS,To}$ is appropriately calibrated for a global-scale study.

We are able to use the regionally-calibrated $Q10_{CS,To}$ globally because CH$_4$ fluxes are observed to have very similar temperature dependencies for a wide range of eco-systems and regions (Yvon-Durocher *et al* 2014). The above mapping approach cannot be directly applied to the NPP substrate-based CH$_4$ emissions relation (JULES-NPP) however, because NPP is itself dependent on soil moisture and temperature. Instead, we calibrate JULES-NPP by comparing against regional fluxes across the optimised JULES-CS (section S2). The resulting values of $Q10_{NPP,To}$ for poor and rich fens, and bogs are 1.3, 1.6 and 2.3, respectively (SI figure S3(c), table S1).

From these comparisons with multiple measurements and models over different spatial and temporal scales, we demonstrate that both the JULES wetland extent and CH$_4$ emission parameterisations respond appropriately to temperature and precipitation and are therefore suitable for the analysis of large-scale CH$_4$ emissions in future climate scenarios.

Climate change simulations

To analyse the potential for wetland CH$_4$ emissions to feedback on climate change, multiple simulations are performed using JULES coupled to a climate change impacts model (IMOGEN, section S5). IMOGEN (Huntingford *et al* 2010) is calibrated against 34 CMIP5 ESM climate simulations (table S6). We perform simulations for 3 RCP GHG scenarios: 2.6, 4.5 and 8.5 (Collins *et al* 2013), which range from a high mitigation strategy to 'business-as-usual'. All GHG concentrations, except for CH$_4$, are prescribed to RCP values, so that interactive wetland CH$_4$ emissions can modify atmospheric CH$_4$ concentration and radiative forcing (section S5, Etminan *et al* 2016). To assess the strength of this wetland CH$_4$-climate feedback, separate simulation sets are carried out with wetland emissions either fixed in time (REF), or able to respond to changes in meteorology.

The atmospheric lifetime of CH$_4$ includes losses from tropospheric OH, stratospheric loss and soil sink, and is also dependent on CH$_4$ concentration as increasing CH$_4$ reduces tropospheric OH (CH$_4$–OH factor *s*, section S5). Myhre *et al* (2013) (3.SM.2) quote contemporary lifetime $\tau_o = 9.25+/0.6$ years and $s = 0.25+/-0.03$. For our control experiment (CTL) we set $\tau_o = 9.25$, $s = 0.25$. To cover uncertainty we add two sensitivity experiments with $\tau_o = 8.65$, $s = 0.22$ and $\tau_o = 9.85$, $s = 0.28$ (section S5).

Both CH$_4$ substrate relations, their $Q10_{To}$'s, and present-day global wetland emissions estimates and their uncertainties, are all considered in the control experiment ensemble (table S1, CTL). (For the purposes of climate simulations here, the lower, median and upper 2000–2009 average wetland flux from current best estimates (Saunois *et al* 2016), are used as the year 2000 LOW, MID and UPP global wetland flux totals, respectively). To investigate uncertainty in modelled physical processes further, additional model ensembles are run without the JULES vegetation-mediated CH$_4$ transfer or tropical soils. We also investigate the impact of: modelled wetland extent errors using an observation-based mask; reduced substrate availability with soil depth; soil carbon uncertainties and; limiting the vegetation flux to Amazonia (sections S3, S4, S7). (Amazonia is the only region where the vegetation flux is studied comprehensively, and measurements from other regions suggest this flux may be smaller elsewhere, Covey and Megonigal 2019).

## Analysing the main feedback drivers and sources of uncertainties

To rigorously assess the relative importance of the drivers of CH$_4$ emission changes, JULES-CS and JULES-NPP, equations (2) and (3) are differentiated as functions of temperature and wetland (and NPP for JULES-NPP) giving:

$$dF_{CH_4}(Cs) \sim F_{CH_4}(Cs)\left(\frac{dfwe}{fwe} + 0.1 \ln(Q10_{CS}(T)) dT \right). \qquad (4)$$

(As we assume a time invariant soil carbon is the main substrate source, Cs is approximated as changing little over the time period considered). For JULES-NPP, equation (3), NPP is not invariant in time, so this differentiates to:

$$dF_{CH_4}(NPP) \sim F_{CH_4}(NPP)\left(\frac{dfwe}{fwe} + 0.1 \ln(Q10_{NPP}(T)) dT + \frac{dNPP}{NPP} \right). \qquad (5)$$

Changes in wetland fraction and precipitation are strongly related (Papa *et al* 2010) so equations (4) and (5) are approximated to:
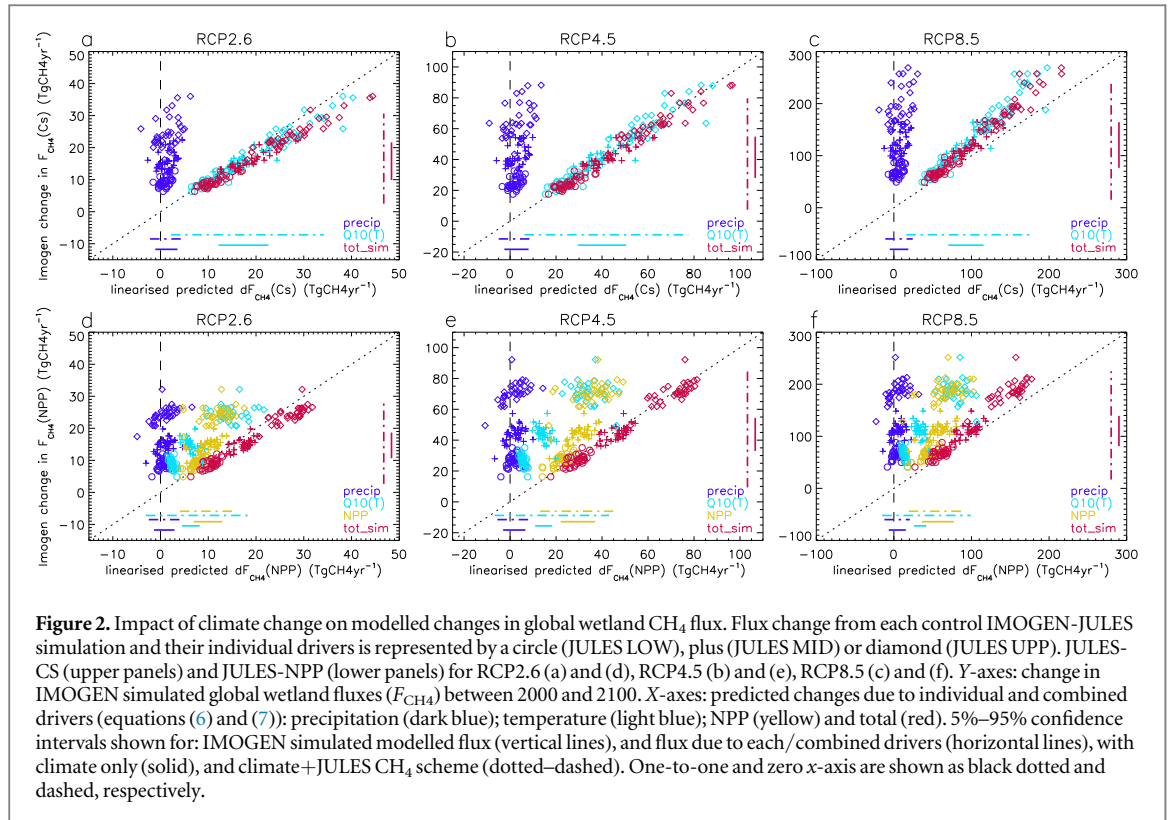
Figure 2. Impact of climate change on modelled changes in global wetland CH$_4$ flux. Flux change from each control IMOGEN-JULES simulation and their individual drivers is represented by a circle (JULES LOW), plus (JULES MID) or diamond (JULES UPP). JULES-CS (upper panels) and JULES-NPP (lower panels) for RCP2.6 (a) and (d), RCP4.5 (b) and (e), RCP8.5 (c) and (f). *Y*-axes: change in IMOGEN simulated global wetland fluxes (F_{CH_4}) between 2000 and 2100. *X*-axes: predicted changes due to individual and combined drivers (equations (6) and (7)): precipitation (dark blue); temperature (light blue); NPP (yellow) and total (red). 5%–95% confidence intervals shown for: IMOGEN simulated modelled flux (vertical lines), and flux due to each/combined drivers (horizontal lines), with climate only (solid), and climate+JULES CH$_4$ scheme (dotted–dashed). One-to-one and zero *x*-axis are shown as black dotted and dashed, respectively.

$$dF_{CH_4}(Cs) \sim F_{CH_4}(Cs)\left(\frac{dprecip}{precip} + 0.1\ln(Q10_{CS}(T))dT\right), \quad (6)$$

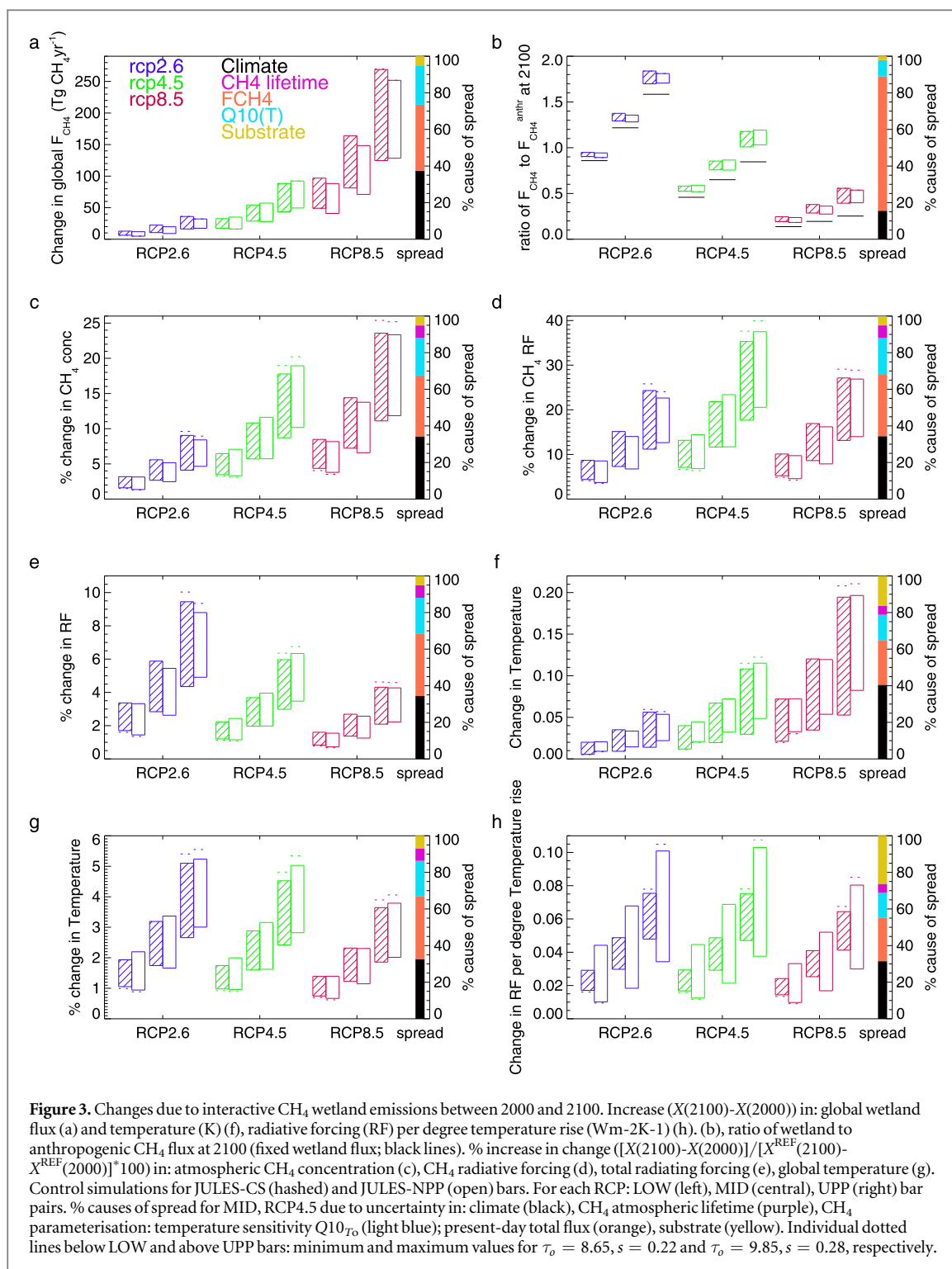$$dF_{CH_4}(NPP) \sim F_{CH_4}(NPP)\left(\frac{dprecip}{precip} + 0.1\ln(Q10_{NPP}(T))dT + \frac{dNPP}{NPP}\right). \quad (7)$$

Results

For the highest GHG scenario RCP8.5, global wetland CH$_4$ emissions are projected to increase from 173 TgCH$_4$yr^{-1} at 2000 to 254–337 TgCH$_4$yr^{-1} and 244–321 TgCH$_4$yr^{-1} by 2100 for MID JULES-CS and JULES-NPP, respectively. A maximum flux of 495 TgCH$_4$yr^{-1} is predicted at 2100 for the 'UPP' estimate (or 494 TgCH$_4$yr^{-1} if only considering the best estimate atmospheric lifetime, table S4, figures 2, 3(a)). Fractional increases in the tropics and extra-tropics are similar (figure S8). Hence future global growth in wetland CH$_4$ flux is dominated by the tropics as this is the main source of present-day emissions.

To understand the causes of these flux changes and their uncertainties, we present the impact of temperature, precipitation and NPP (light and dark blue and yellow symbols, respectively; figure 2) on global CH$_4$ flux changes (equations (6) and (7)). Wetland extent responses are dominated by differences in precipitation

projections (as demonstrated by comparing figures 2 and S7) which are themselves highly uncertain. Consequently the simulations do not predict a consistent expansion or contraction over most wetland regions (figures 1(g) and (h)). There is even a lack of consensus as to whether the global total wetland area is likely to increase or decrease in the future. (For example, for RCP8.5 simulations it varies from a 2% decrease to a 19% increase between 2000 and 2100). Hence projected changes in precipitation result in simulated CH$_4$ flux changes of uncertain sign. The resulting flux changes are of relatively small magnitude however. Projected temperature change is a more important driver than precipitation, and results in both a larger CH$_4$ flux response and a greater uncertainty (figure 2). For JULES-NPP, some of the temperature response is within the NPP term. As well as being dependent on temperature, NPP is also strongly driven by atmospheric CO$_2$ (through increased CO$_2$ fertilisation), which is in itself highly correlated with temperature.

In both substrate parameterisations the spread in projected wetland CH$_4$ flux by year 2100 is dominated by uncertainty in the wetland emissions parameterisation (figure 3). The uncertainty due to simulated climate change (within a specific RCP) plays a smaller, but still significant role (63%–65% versus 35%–37% over the three RCP scenarios—only RCP4.5 shown in figure 3(a)). Within the wetland scheme, uncertainty due to present-day global wetland flux estimate is larger than that from temperature sensitivity ($Q10_{To}$, figure 3(a)). Moreover the projected spread due to global present-day wetland emissions uncertainty alone is

Figure 3. Changes due to interactive CH_4 wetland emissions between 2000 and 2100. Increase ($X(2100)-X(2000)$) in: global wetland flux (a) and temperature (K) (f), radiative forcing (RF) per degree temperature rise (Wm-2K-1) (h). (b), ratio of wetland to anthropogenic CH_4 flux at 2100 (fixed wetland flux; black lines). % increase in change ([$X(2100)-X(2000)$]/[$X^{REF}(2100)-X^{REF}(2000)$]*100) in: atmospheric CH_4 concentration (c), CH_4 radiative forcing (d), total radiating forcing (e), global temperature (g). Control simulations for JULES-CS (hashed) and JULES-NPP (open) bars. For each RCP: LOW (left), MID (central), UPP (right) bar pairs. % causes of spread for MID, RCP4.5 due to uncertainty in: climate (black), CH_4 atmospheric lifetime (purple), CH_4 parameterisation: temperature sensitivity $Q10_{T_o}$ (light blue); present-day total flux (orange), substrate (yellow). Individual dotted lines below LOW and above UPP bars: minimum and maximum values for $\tau_o = 8.65, s = 0.22$ and $\tau_o = 9.85, s = 0.28$, respectively.

comparable to that from simulated climate change. Critically, in terms of CH_4 generation process uncertainty, the impact of substrate source used (i.e. Cs versus NPP), is relatively small (between 5% and 13% for the different scenarios). We also find that the wetland physics sensitivity experiments have little impact on the projected future wetland flux (section S7).

Enhanced wetland CH_4 emissions cause substantial 21st century increases in atmospheric CH_4 concentration of up to 25.4% above that with fixed wetland emissions (and 23.6% without including the CH_4 atmospheric lifetime sensitivity experiments) (figures 3(c) and 4). Depending on the scenario, the corresponding 21st century increases in total and CH_4 radiative forcings are further enhanced by between 0.7%–10.0% and 3.5%–40.0%, respectively. The percentage changes in CH_4 radiative forcing are higher for lower RCP scenarios (figures 3(c) and (d)) because CH_4 radiative forcing is nonlinearly dependent on concentration (Etminan *et al* 2016). This radiative
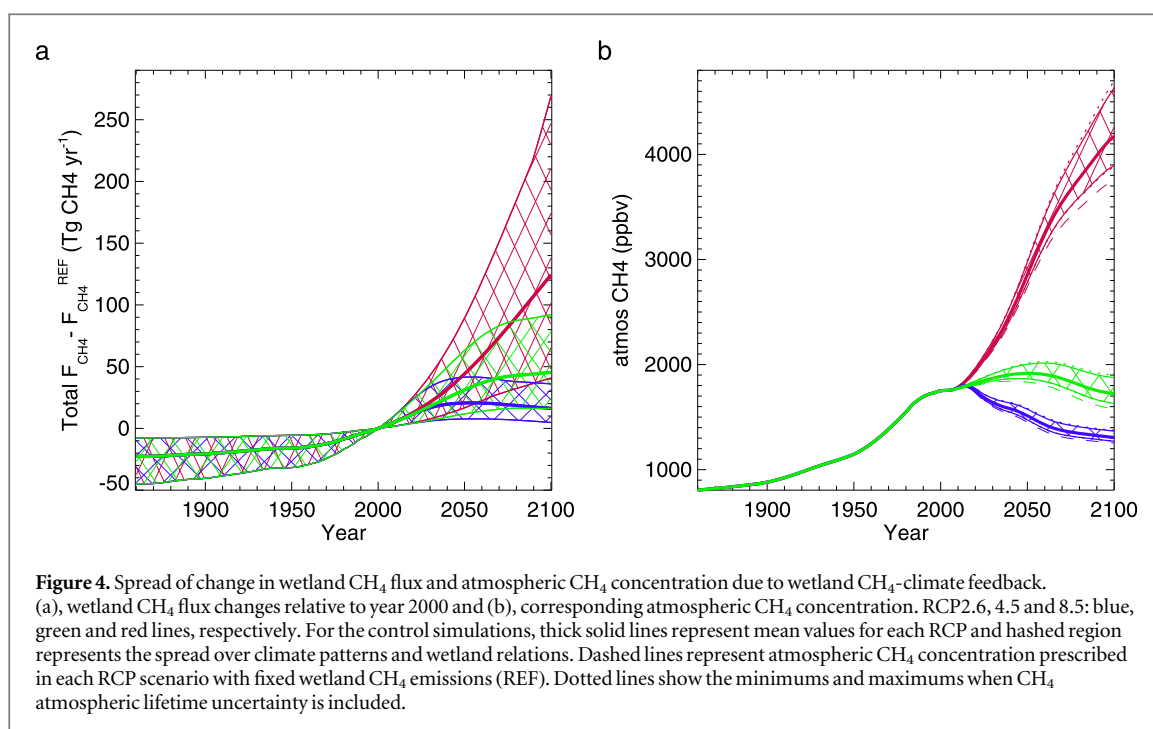
Figure 4. Spread of change in wetland CH_4 flux and atmospheric CH_4 concentration due to wetland CH_4-climate feedback. (a), wetland CH_4 flux changes relative to year 2000 and (b), corresponding atmospheric CH_4 concentration. RCP2.6, 4.5 and 8.5: blue, green and red lines, respectively. For the control simulations, thick solid lines represent mean values for each RCP and hashed region represents the spread over climate patterns and wetland relations. Dashed lines represent atmospheric CH_4 concentration prescribed in each RCP scenario with fixed wetland CH_4 emissions (REF). Dotted lines show the minimums and maximums when CH_4 atmospheric lifetime uncertainty is included.

Table 1. Reduction in allowed anthropogenic (fossil fuel and land use related) emissions between 2020 and 2100 due to wetland CH_4-climate feedback. Average, and range of 68% probability (mean and $+/-1$ standard deviation) shown in brackets. The values are based on the control and CH_4 atmospheric lifetime sensitivity experiments.

	RCP2.6	RCP4.5	RCP8.5
Remaining anthr emissions (without wetland–CH_4 feedback)	268.2	661.4	1809.3
Reduction (GtC)	21.4 (12.4–30.4)	36.7 (21.6–51.9)	79.1 (45.0–113.2)
Reduction as % of remaining	8.0 (4.6–11.3)	5.6 (3.3–7.8)	4.4 (2.5–6.3)

forcing enhancement leads to an additional increase in global air temperature of up to 0.21 K at 2100 (and land air temperature of up to 0.27 K -not shown).

The relative causes of uncertainty in the enhanced total radiative forcing and percentage temperature changes are similar to those in wetland emissions (figure 3). In addition, atmospheric CH_4 lifetime uncertainty contributes around 7% of the total spread in radiative forcing and temperature changes.

Due to wetland emissions feedback, significant reductions in allowed anthropogenic emissions are required to maintain projected temperature changes between 2020 and 2100 (appendix SB, table 1). For RCP2.6 these reductions are 21.4 GtC, with a likely value (greater than 68% probability) of between 12.4–30.4 GtC (4.6%–11.3%). This is consistent with the Comyn-Platt *et al* (2018) estimate of 19.6 GtC for the comparable 1.5 °C stabilisation threshold. (This is despite Comyn-Platt *et al* 2018 using a different substrate generation scheme, thereby further demonstrating that the impact of substrate used is relatively small). Near-term implications are significant with the RCP2.6 mid 21st century global temperature peak reached nine years earlier (4–16 years) (not shown).

CH_4 emissions from wetlands increase significantly from present day to 2100 in all simulated

climate change patterns and RCP scenarios. In the higher sensitivity wetland emission relation, they may more than double between 2000 and 2100, with an associated change in atmospheric CH_4 concentration of up to 952 ppbv (figure 4). The subsequent feedback on radiative forcing ranges from 0.01 to 0.11 $Wm^{-2} K^{-1}$. Despite the improved physical representation in JULES, this has little impact on the feedback magnitude of the wetland emissions on climate at the global scale (section S7).

Discussion and conclusions

There is also considerable uncertainty in other inland water CH_4 source emissions (Saunois *et al* 2016) and these are also likely to respond to climate change (Ciais *et al* 2013). Present-day rice agriculture emissions are estimated to be around 36 $TgCH_4yr^{-1}$ which is between 16% and 30% of natural wetland emission estimates (Saunois *et al* 2016). Moreover, even without rice agriculture expanding, their associated CH_4 emissions are likely to increase in response to temperature (Khalil *et al* 1998), adding an additional radiative feedback.

We have included new physical processes: the CH_4 transfer through tropical trees and the inclusion of tropical-specific soils, to improve wetland representation

in this important region. This allows us to make more accurate assessments of the feedback magnitude between wetland CH_4 release and climate change. We have determined this feedback uncertainty by constraining wetland parameterisations, using data from multiple sources over local to regional scales. Despite this, there remains a sizeable feedback uncertainty, which is dominated by relatively poorly known wetland extent and CH_4 parameters, rather than that due to climate change. Our more rigorous and constrained approach helps explain the IPCC's assessment of 'low confidence' in the magnitude of the wetland CH_4-climate feedback (Ciais *et al* 2013). Furthermore, we identify the main causes of the uncertainty range, which can be further constrained through future measurement campaigns focusing on detailed wetland processes, including those determining the vegetation transport of CH_4 (Covey and Megonigal 2019). Given that the remaining lack of knowledge in contemporary global wetland CH_4 flux is the single largest cause of wetland scheme uncertainty, improved estimates of present-day global wetland emissions remain a research priority.

The CH_4 feedback on climate may be enhanced or reduced through interactions with other parts of the earth system through the intricate coupling of biogeochemical cycling and reactive atmospheric chemistry. For instance, we do not consider the interaction with the carbon cycle in which changing atmospheric CO_2 and climate may alter the size and distribution of vegetation and soil carbon, and in turn the available substrate for methanogenesis. Understanding these interactions, and their potential nonlinearities, will become possible as the processes analysed in this study are routinely incorporated in to the next generation of ESM, and we suggest this should be a priority.

Under a range of future socio-economic assumptions, from high GHG emission mitigation to 'business-as-usual' scenarios, we find that wetland CH_4 feedbacks in a warming climate will significantly augment atmospheric CH_4 concentrations by up to 25.4% over the 21st century. This raises CH_4 radiative forcing significantly beyond that caused by direct human activity, producing a positive feedback that further enhances climate change. Over the scenarios considered, the wetland feedback amplifies the 21st century CH_4 radiative forcing on average by 14.4%, with uncertainty estimates indicating values as high 40.0% for the RCP4.5 scenario. This generates an average additional warming of 2.4%. Under the RCP2.6 emissions scenario (which gives an approximately 1.5 °C increase in temperature from pre-industrial to 2100), the 21st century temperature rise is amplified by up to 5.5%, and furthermore rises more quickly in the near term. This corresponds to a likely reduction in remaining allowed anthropogenic emissions of between 4.6%–11.3% in order to maintain the same temperature profiles. The more rapid warming and carbon budget reduction, imply that a combination of enhanced short-term emission cuts and longer-term

increased use of negative emission technology, are required to be consistent with the Paris climate targets.

ORCID iDs

N Gedney ⓘ https://orcid.org/0000-0002-2165-5239

References

Arneth A *et al* 2010 Terrestrial biogeochemical feedbacks in the climate system *Nat. Geosci.* **3** 525–32

Best M J *et al* 2011 The joint UK land environment simulator (JULES), model description: I. Energy and water fluxes *Geosci. Model Dev.* **4** 677–99

Bridgham S D *et al* 2013 Methane emissions from wetlands: biogeochemical, microbial, and modeling perspectives from local to global scales *Glob. Change Biol.* **19** 1325–46

Ciais P *et al* 2013 *Climate Change 2013: The Physical Science Basis* ed T F Stocker *et al* (Cambridge: Cambridge University Press) ch 6 pp 465–570

Clark D B *et al* 2011 The joint UK land environment simulator (JULES), model description: II. Carbon fluxes and vegetation dynamics *Geosci. Model Dev.* **4** 701–22

Collins M *et al* 2013 *Climate Change 2013: The Physical Science Basis* ed T F Stocker *et al* (Cambridge: Cambridge University Press) ch 12 pp 1029–136

Comyn-Platt E *et al* 2018 Carbon budgets for 1.5 °C and 2 °C targets lowered by natural wetland and permafrost feedbacks *Nat. Geosci.* **11** 568–73

Covey K R and Megonigal J P 2019 Methane production and emissions in trees and forests *New Phytol.* **222** 18–28

Davidson N C *et al* 2018 Global extent and distribution of wetlands: trends and issues *Mar. Freshwater Res.* **69** 620–7

Etminan M *et al* 2016 Radiative forcing of carbon dioxide, methane, and nitrous oxide: a significant revision of the methane radiative forcing *Geophys. Res. Lett.* **43** 12614–23

Gedney N and Cox P M 2003 The sensitivity of global climate model simulations to the representation of soil moisture heterogeneity *J. Hydromet.* **4** 1265–75

Gedney N, Cox P M and Huntingford C 2004 Climate feedback from wetland methane emissions *Geophys. Res. Lett.* **31** L20503

Huntingford C *et al* 2010 IMOGEN: an intermediate complexity model to evaluate terrestrial impacts of a changing climate *Geosci. Model Dev.* **3** 679–87

Khalil M A K *et al* 1998 Factors affecting methane emissions from rice fields *J. Geophys. Res.* **103** 219–25

Kirschke S *et al* 2013 Three decades of global methane sources and sinks *Nat. Geosci.* **6** 813–23

Marthews T R *et al* 2014 High-resolution hydraulic parameter maps for surface soils in tropical South America *Geosci. Model Dev.* **7** 711–23

McNorton J *et al* 2016 Role of regional wetland emissions in atmospheric methane variability *Geophys. Res. Lett.* **43** 11433–44

Megonigal J P *et al* 1999 A plant-soil-atmosphere microcosm for tracing radiocarbon from photosynthesis through methanogenesis *Soil Sci. Soc. Am. J.* **63** 665–71

Melton J R *et al* 2013 Present state of global wetland extent and wetland methane modelling: conclusions from a model inter-comparison project (WETCHIMP) *Biogeosciences* **10** 753–88

Myhre G *et al* 2013 *Climate Change 2013: The Physical Science Basis* ed T F Stocker *et al* (Cambridge: Cambridge University Press) ch 8 pp 659–740

Nachtergaele F and Batjes N 2012 *Harmonized world soil database* (Rome: FAO)

Nisbet E G, Dlugokencky E J and Bousquet P 2014 Methane on the rise-again *Science* **343** 493–5

Pangala S R *et al* 2017 Large emissions from floodplain trees close the Amazon methane budget *Nature* **552** 230–4

Papa F *et al* 2010 Interannual variability of surface water extent at the global scale, 1993–2004 *J. Geophys. Res.* **115** D12111

Poulter B *et al* 2017 Global wetland contribution to 2000-2012 atmospheric methane growth rate dynamics *Env. Res. Lett.* **12** 094013

Riley W J *et al* 2011 Barriers to predicting changes in global terrestrial methane fluxes: analyses using CLM4Me, a methane biogeochemistry model integrated in CESM *Biogeosciences* **8** 1925–53

Roulet N T *et al* 1992 Northern fens: methane flux and climate change *Tellus* B **44** 100–5

Saunois M *et al* 2016 The global methane budget: 2000–2012 *Earth Syst. Sci. Data* **8** 1–54

Stocker B D *et al* 2013 Multiple greenhouse-gas feedbacks from the land biosphere under future climate change scenarios *Nat. Clim. Change* **3** 666–72

Turetsky M R *et al* 2014 A synthesis of methane emissions from 71 northern, temperate, and subtropical wetlands *Glob. Change Biol.* **20** 2183–97

Weedon G P *et al* 2014 The WFDEI meteorological forcing data set: WATCH forcing data methodology applied to ERA-Interim reanalysis data *Wat. Resour. Res.* **50** 7505–14

Yvon-Durocher G *et al* 2014 Methane fluxes show consistent temperature dependence across microbial to ecosystem scales *Nature* **507** 488–91